Int. J. Heat Mass Transfer. Vol. 30, No. 2, pp. 215-222, 1987
Printed in Great Britain

0017-9310/87 $3.00+0.00
Pergamon Journals Ltd.

Evaporative mass transfer in turbulent forced convection duct flows

W. CHUCK and E. M. SPARROW
Department of Mechanical Engineering, University of Minnesota, Minneapolis, MN 55455, U.S.A.

(*Received* 24 *March* 1986 *and in final form* 9 *June* 1986)

Abstract—Experiments were performed to determine the mass transfer characteristics for evaporation from partially filled pans of distilled water recessed in the floor of a flat rectangular duct through which turbulent air flow was passed. During the course of the experiments, parametric variations were made of the Reynolds number of the air flow, the streamwise length of the pan, and the distance between the top of the pan and the water surface (hereafter referred to as the step height). For all of the operating conditions of the experiments, the measured Sherwood numbers were well correlated with the Reynolds number provided that the step height was used as the characteristic dimension. Guided by analytical considerations, a second correlation was constructed which provides Sherwood number predictions for operating conditions corresponding to pans longer than those used in the present experiments. By making use of the analogy between heat and mass transfer, it was shown how Nusselt numbers can be obtained from the Sherwood number correlations.

INTRODUCTION

THE EVAPORATIVE mass transfer problem to be investigated here is conveniently described by reference to the schematic diagram presented in Fig. 1. That diagram is a longitudinal-sectional view showing a partially filled pan of water situated in the lower wall of a flat rectangular duct. A hydrodynamically developed, turbulent air flow is delivered by the duct to the upstream end of the pan, where it encounters a step-change increase in cross-section which causes separation to occur. The separated flow may reattach either at the water surface or at the downstream wall of the pan that is exposed above the water level, depending on the length–height ratio L/h of the cavity-like space above the water surface. In either case, evaporation takes place at the water surface, causing an increase in the water vapor content of the air flow.

The investigation was primarily experimental, and its main focus was to determine mass transfer coefficients and Sherwood numbers for the evaporation process. Two dimensionless parameters were varied during the course of the experiments. These included the duct Reynolds number, which ranged between 7200 and 21,000, and the length–height ratio L/h of the cavity above the water surface. To obtain an extensive range for the L/h ratio, pans having two different streamwise lengths were employed. The shorter of the pans yielded results for L/h between 8 and 25, while the longer pan provided results for L/h between 18 and 55.

Two types of correlations were devised to generalize the experimental results. The first serves as an interpolation formula among the investigated operating conditions for the two pans. The second correlation, whose structure was guided by analytical considerations, was based on the results for the longer of the pans and serves as an extrapolation formula from which results for still longer pans can be obtained.

Although the results presented here are couched in terms of the Sherwood number, they may equally well be regarded as Nusselt numbers, in accordance with the well-established analogy between heat and mass transfer. Since the Schmidt number for the present mass transfer experiments is 0.6, the corresponding Nusselt numbers pertain to a Prandtl number of 0.6. To scale the Nusselt number results to other Prandtl numbers such as 0.7 (heat transfer in air), a power law such as $Pr^{0.4}$ may be used.

A survey of the literature failed to reveal prior evaporative mass transfer experiments of the type performed here. The survey was then extended to the analogous problem of heat transfer at the walls of open-topped cavities. For that problem, the only available experimental information is for cavities which open onto external flows (e.g. [1–6]), rather than onto duct flows as in the present investigation. The literature information suggests that for cavities with L/h ratios greater than 8, the separated flow will reattach at the floor of the cavity. On the other hand, when the ratio is less than 8, the reattachment will occur at the downstream wall of the cavity.

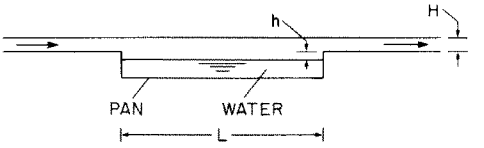

FIG. 1. Longitudinal-sectional view of the test section and of the adjacent portions of the rectangular duct.

NOMENCLATURE

A	planform area, wL
D	hydraulic diameter of flow cross-section of mass transfer section
$\mathscr{D}$	mass diffusion coefficient
H	duct height
h	distance between water surface and top of pan (step height)
K	average mass transfer coefficient, equation (13)
L	streamwise length of pan
M	molecular weight
$\dot{m}$	mass flow rate
$\dot{m}_{evap}$	rate of evaporation from water surface
P	perimeter of flow cross-section of mass transfer section
Pr	Prandtl number
p	pressure
Q	volumetric flow rate
R	gas constant
Re_D	hydraulic-diameter Reynolds number, $4\dot{m}/\mu P$
Re_h	step-height Reynolds number, $\bar{u}_1 h/\nu$
Sc	Schmidt number
Sh_D	average Sherwood number based on D, $KD/\mathscr{D}$
$Sh_{D,fd}$	fully developed Sherwood number
Sh_h	average Sherwood number based on h, $Kh/\mathscr{D}$
Sh_{PP}	fully developed Sherwood number from Petukhov–Popov correlation
T	temperature
$\bar{u}_1$	mean velocity in duct upstream of mass transfer section
W	specific humidity
W	width of duct cross-section
w	width of pan.

Greek symbols

$\Delta\rho_w$	log-mean density difference of water vapor
μ	viscosity
ν	kinematic viscosity
ρ	density.

Subscripts

a	dry air
rot	at the rotameter
s	at the water surface
std	at standard conditions
w	water vapor
1	in the duct just before the mass transfer section
2	in the duct just after the mass transfer section.

EXPERIMENTS

Apparatus

The description of the experimental apparatus is facilitated by following the path of the air flow. Air from the temperature-controlled laboratory room was drawn via a sharp-edged inlet into a flat rectangular duct having a 4.3:1 cross-sectional aspect ratio (width × height). As it passed through the 33.3-hydraulic-diameters-long portion of the duct upstream of the test section, the flow became hydrodynamically developed as witnessed by pressure drop linearity. The test section was actually a continuation of the duct but with the lower wall replaced by a rectangular pan which served to contain the evaporating distilled water. The upper wall of the test section was made of plexiglass to enable the water surface to be observed. Both the containment pan and the plexiglass upper wall were designed to be removed from (or incorporated into) the test section in a matter of seconds, with the rapid disassembly (or assembly) being facilitated by the use of quick-release clamps. Positive sealing against leaks was achieved by the use of O-ring material.

The rectangular duct continued well downstream of the test section. From the duct exit, the air successively passed through a rectangular-to-circular transition piece, a flowmeter, a control valve, and a blower. The blower was situated in a service corridor adjacent to the laboratory, and its compression-heated, water-vapor-enriched discharge was vented outside the building.

Figure 1 displays a longitudinal-sectional view of the test section and of the adjacent portions of the rectangular duct. Schematic cross-sectional views of the test section and of the duct are respectively presented in Figs. 2(a) and (b). The duct had cross-sectional dimensions H and W equal to 1.928 and 8.275 cm, while the distance h between the surface of the water and the top of the pan was one of the variables of the experiments.

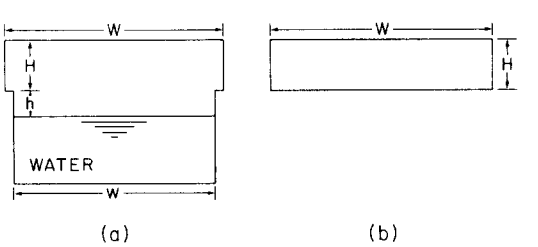

FIG. 2. Cross-sectional views of (a) the test section and (b) the rectangular duct.

As noted earlier, pans having two different streamwise lengths L were used during the course of the experiments, 12.502 and 27.915 cm, respectively. Both pans were fabricated from aluminum, which was chosen because its low density enabled the weight of the pan and the water it contained to be kept within the 2610 g range of an available, highly accurate (0.1 g) triple-beam balance. To avoid electrochemical interactions between the water and the aluminum, the interior walls of the pan were coated with epoxy paint whose surface was made smooth by hand polishing.

The respective pans had a depth of 3.665 cm when empty, with a width of 7.582 cm that was slightly less than the 8.275 cm width of the duct [see Fig. 2(a)]. The slight difference in widths was necessitated by the method used to mate the pan with the duct side walls. Because of the greater width of the duct, the surface of the water was not washed by the duct side-wall boundary layers.

The rectangular duct was also made from aluminum. Before assembly of the duct, all interior surfaces were polished to ensure hydrodynamic smoothness. O-Ring material was used to seal against leaks.

Instrumentation and experimental procedure

Attention will now be turned to the instrumentation. The rate of evaporative mass transfer was determined from the change of mass of the distilled water in the pan during a preselected interval of time, with the mass being measured both immediately before and immediately after the interval. To accomplish these measurements, the pan was removed from the test section and placed on the weighing platform of the aforementioned triple-beam balance. In order to avoid any possible extraneous loss of mass during this operation (e.g. due to spillage), especially when the pan was nearly full, a special fixture was fabricated which enabled the weighing to be performed by lowering the pan only a fraction of an inch beneath its installed position in the duct [7].

A total of 15 thermocouples were installed in the pan for the measurement of the water surface temperature. In this regard, the rectangular planform area wL of the water surface was subdivided into 15 equal-area rectangles and a thermocouple junction placed at the center of each rectangle. The thermocouples were further positioned so that their junctions were, on the average, about 0.125 cm beneath the surface of the water. The thermocouples were fabricated from Teflon-coated, 0.0254-cm-diameter chromel and constantan wire. This choice was made because of the high thermoelectric output of chromel–constantan thermocouples and because neither chromel, constantan, nor Teflon react with water. Thermocouples were also installed in the duct cross-section both upstream and downstream of the test section. The thermocouple wire had been calibrated specifically for these experiments. The e.m.f.s of the thermocouples were read with a digital voltmeter having a resolution of 1 μV.

The moisture content of the air entering the rectangular duct was measured by an aspiration-type psychrometric unit situated adjacent to the duct inlet. It was fabricated from a 76.2-cm length of 7.62-cm-i.d. plexiglass tubing, with an aspirating fan installed at the downstream end. The air velocity resulting from the fan CFM and the cross-sectional area of the tube yielded near equality of the psychrometric wet-bulb temperature and the adiabatic saturation temperature.

Two mercury-in-glass thermometers, capable of being read to 0.1°F or better, were installed in the plexiglass tube one behind the other in crossflow, with a separation distance of about 30 thermometer diameters. The bulbs of the thermometers were centered at the tube axis. The upstream thermometer was used for the dry-bulb temperature measurement and the downstream thermometer for the wet-bulb temperature measurement. To minimize radiation effects, the plexiglass tube was covered with a sheet of aluminum foil.

A height gage was designed and fabricated to measure the distance h between the surface of the water and the top of the pan [7]. With the upper wall of the test section removed and the air flow deactivated, the gage was suspended over the upstream end of the pan by a bridge-like fixture supported by the side walls of the test section. For the measurement, the sensing tip of the gage was first brought into contact with the floor of the duct, and the reading of a micrometer head was noted and recorded. Then, the sensing tip was brought into contact with the water surface, and the micrometer was read again. These two readings were differenced to yield the height h. To ensure accurate detection of contact, the sensing tip was made part of an electrical circuit whose closure was indicated by the deflection of the needle of an analog-type voltmeter.

Pressure taps were provided immediately upstream and downstream of the test section and at the flowmeter, and a precision barometer was used for the ambient pressure. Either of two calibrated rotameters was used for the volumetric flow measurement, depending on the magnitude of the flow rate.

In the execution of the experiments, each evaporation run was preceded by an equilibration period of approximately an hour. The depth h and the mass of the water-filled pan were measured immediately before and immediately after the run. During the run, three separate sets of data were collected for the water temperature (15 thermocouples), the air temperatures in the duct, the wet- and dry-bulb temperatures in the psychrometric unit, the float position in the rotameter, and the barometric pressure in the laboratory room. The static pressures were measured once—midway in the run. Typically, the duration of an evaporation run was either 1 or $1\frac{1}{2}$ h, depending on the evaporation rate.

DATA REDUCTION

The main objective of the data reduction was to evaluate the Sherwood and Reynolds numbers from the experimental data. Since a knowledge of the specific humidity W is a prerequisite for the evaluation of both of these groups, it will be considered first.

The specific humidity of the air at the duct inlet was calculated from the measured wet- and dry-bulb temperatures and the barometric pressure, in conjunction with psychrometric equations widely available in standard textbooks (e.g. [8, pp. 393–395]). The details of the calculations, including curve fits of the needed thermodynamic properties, are set forth in ref. [7].

Specific humidities are needed at three other stations designated as follows:

1 just upstream of the test section
2 just downstream of the test section
rot at the rotameter.

Since there is no mass transfer between the duct inlet and the upstream end of the test section, the specific humidity is a constant between these two stations. Therefore, W_1 is known from the aforementioned calculation of the inlet-section specific humidity.

For W_2, a mass balance across the test section yields (ignoring negligible time-dependent effects)

$$W_2 = W_1 + (\dot{m}_{evap}/\dot{m}_a). \tag{1}$$

In this equation, $\dot{m}_{evap}$ is the rate of evaporation of water vapor from the liquid surface into the air stream. Its numerical value was obtained by ratioing the measured change of mass of the liquid in the containment pan with the duration of the evaporation period. The quantity $\dot{m}_a$ is the flow rate of dry air passing through the system, which is independent of position but unknown.

Since the mass flow rate will be evaluated at the rotameter, it is convenient to express $\dot{m}_a$ in terms of $\dot{m}_{rot}$, where

$$\dot{m}_{rot} = \dot{m}_a + \dot{m}_{w,rot} = \dot{m}_a(1 + W_{rot}). \tag{2}$$

The flow rate $\dot{m}_w$ of the water vapor varies along the test section but is a constant between the downstream end of the test section and the rotameter. As a consequence

$$W_{rot} = W_2 \tag{3}$$

and equation (1) becomes

$$W_2 = W_1 + (1 + W_2)(\dot{m}_{evap}/\dot{m}_{rot}). \tag{4}$$

To proceed, it is necessary to consider the details of the determination of $\dot{m}_{rot}$. As is well known, a rotameter indicates the volumetric flow rate at standard conditions. In practice, the indicated volumetric flow rate Q_{std} has to be converted to the actual flow rate Q_{rot} which corresponds to the thermodynamic state of the fluid passing through the rotameter, i.e.

$$Q_{rot} = Q_{std}(\rho_{std}/\rho_{rot})^{1/2} \tag{5}$$

and for $\dot{m}_{rot}$, there follows

$$\dot{m}_{rot} = \rho_{rot} Q_{rot} = Q_{std}(\rho_{std}\rho_{rot})^{1/2}. \tag{6}$$

For a mixture of air and water vapor with a specific humidity W_{rot}, it can be easily shown that

$$\rho_{rot} = \{(1 + W_{rot})/[1 + W_{rot}(M_a/M_w)]\} \times (p_{rot}/R_a T_{rot}) \tag{7}$$

in which p_{rot} and T_{rot} are the pressure and temperature at the rotameter (both of which are known), M_a and M_w are the molecular weights of air and water vapor, and R_a is the gas constant of air. Note also that

$$\rho_{std} = p_{std}/R_a T_{std}. \tag{8}$$

If equations (7) and (8) are substituted into (6) which is, in turn, introduced into equation (4), there results a quadratic equation in which W_2 ($= W_{rot}$) is the only unknown. This enabled numerical determination of W_2 and, subsequently, of $\dot{m}_{rot}$ from equations (6)–(8). Note that $\dot{m}_2 = \dot{m}_{rot}$ and that

$$\dot{m}_1 = [(1 + W_1)/(1 + W_2)]\dot{m}_2. \tag{9}$$

It is relevant to note that for all the operating conditions of the experiments, the maximum deviation between $\dot{m}_1$ and $\dot{m}_2$ was 0.05%. In view of this, no further distinction will be made between $\dot{m}_1$ and $\dot{m}_2$ and, instead, the single symbol $\dot{m}$ will be used to denote the mass flow rate.

Two Reynolds numbers will be used in the presentation of results. One of these will be designated as the step-height Reynolds number Re_h in that the characteristic dimension is the downstep distance h between the top of the containment pan and the water surface. The definition of Re_h to be used here is

$$Re_h = \bar{u}_1 h/\nu \tag{10}$$

in which $\bar{u}_1$ is the mean velocity in the duct just upstream of the test section.

The second Reynolds number is a conventional hydraulic-diameter Reynolds number based on the flow cross-section dimensions of the test section, i.e. the flow cross-section pictured in Fig. 2(a). This Reynolds number will be denoted by Re_D ($D \sim$ hydraulic diameter) and expressed as

$$Re_D = 4\dot{m}/\mu P \tag{11}$$

in which P is the entire perimeter of the flow cross-section of the test section

$$P = 2(W + H + h). \tag{12}$$

The viscosity used in evaluating equations (10) and (11) was that of pure air, since the effect of moisture on viscosity is negligible at atmospheric pressure.

For the Sherwood number, the first step is to evaluate a mass transfer coefficient K

$$K = \dot{m}_{evap}/A(\Delta\rho_w). \tag{13}$$

Here, A is the planform area wL, and $\Delta\rho_w$ is the log-mean density difference of the water vapor

$$\Delta\rho_w = (\rho_{w1}-\rho_{w2})/\ln[(\rho_{ws}-\rho_{w2})/(\rho_{ws}-\rho_{w1})] \quad (14)$$

in which ρ_{w1}, ρ_{w2} and ρ_{ws} are the partial densities of water vapor just upstream of the test section, just downstream of the test section, and at the surface of the water. The use of the arithmetic-mean density difference yielded results that were indistinguishable from those based on the log-mean density difference.

To determine ρ_{w1}, it may be noted that

$$\rho_{w1} = p_{w1}/R_w T_1, \quad p_{w1} = p_1/[1+W_1(M_w/M_a)] \quad (15)$$

in which T_1 and p_1 are measured quantities, and W_1 is known, as previously described. Similar equations are used for evaluating ρ_{w2}. For ρ_{ws}, it was assumed that phase equilibrium exists at the surface of the evaporating water. Consequently, ρ_{ws} was evaluated as the saturation density corresponding to the surface temperature of the water.

In common with the Reynolds number, two Sherwood numbers will be used in presenting the results. One, the step-height Sherwood number, is defined as

$$Sh_h = Kh/\mathscr{D} \quad (16)$$

while the other is the hydraulic-diameter Sherwood number Sh_D given by

$$Sh_D = KD/\mathscr{D} \quad (17)$$

where

$$D = 4(HW+hw)/2(W+H+h). \quad (18)$$

In these equations, $\mathscr{D}$ is the mass diffusion coefficient for mixtures of air and water vapor, the values of which were taken from ref. [9].

RESULTS AND DISCUSSION

The presentation of results has two objectives. The first is to correlate the Sherwood number results for all the investigated operating conditions for the two pans. Such a correlation will serve as an interpolation formula among the discrete values of the parameters employed in the experiments. The second objective is to construct a correlation which will predict Sherwood numbers for operating conditions corresponding to pans that are longer than those used here.

To fulfill the first objective, a Sherwood–Reynolds correlation was sought using various definitions of the Sherwood and Reynolds numbers. In one definition, the characteristic dimension was the hydraulic diameter of the $H \times W$ cross-section of the rectangular duct. In a second, the characteristic dimension was the hydraulic diameter of the flow cross-section of the mass transfer section, giving rise to the Re_D and Sh_D of equations (11) and (17). In a third, the Sherwood and Reynolds numbers involved the streamwise length L of the pan. The fourth definition was based on the step height h as the characteristic dimension, leading to the Re_h and Sh_h of equations (10) and (16). As documented in ref. [7], neither of the first three options successfully correlated the data for both the shorter and longer pans. On the other hand, as will now be demonstrated, the fourth option leads to a satisfactory correlation, which will subsequently be modified to yield a uniformly good representation of the data.

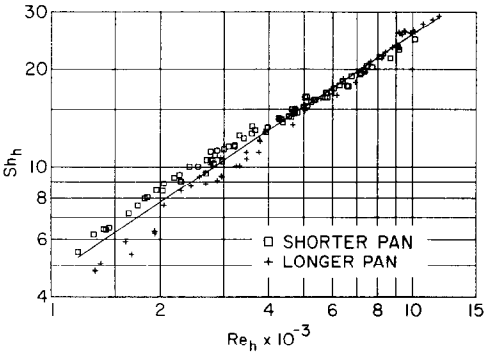

FIG. 3. Correlation of the step-height Sherwood and Reynolds numbers for all the operating conditions of the experiments.

Figure 3 displays the mass transfer data for both pans in the Sh_h vs Re_h format, with square symbols used for the shorter pan and cross symbols for the longer pan. The aggregate data covers the Re_h range from about 1200 to 12,000. In addition to the data, Fig. 3 contains a least-squares, power-law fit expressed by

$$Sh_h = 0.0285Re_h^{0.738}. \quad (19)$$

Inspection of the figure reveals that for $Re_h > 3800$, the data for both pans are very well correlated and display only a few percent spread with respect to equation (19). On the other hand, when $Re_h < 3800$, the data for the respective pans tend to separate, with those for the shorter pan falling above the correlating line and those for the longer pan falling below. However, even in this range of Re_h, the deviations of the shorter-pan data from the line are generally less than 10%. The same is true for the longer-pan data for Re_h down to about 2000, and only at lower Re_h do greater deviations occur.

The foregoing discussion suggests that equation (19) is a satisfactory representation of the data. However, a tighter correlation can be achieved if another characteristic dimension is used in addition to the step height h. The most promising approach was to include the factor $(L/h)^m$ in the Sh_h–Re_h power-law representation. A least-squares fit of the data with this factor in place yielded

$$Sh_h = 0.0470Re_h^{0.711}/(L/h)^{0.0968}. \quad (20)$$

A graphical display of the correlation is presented in Fig. 4, where $Sh_h(L/h)^{0.0968}$ is plotted vs Re_h. From the figure, it is seen that the deviations of the data relative to the correlating line are now relatively uniform over the entire investigated range of Re_h. About two-thirds

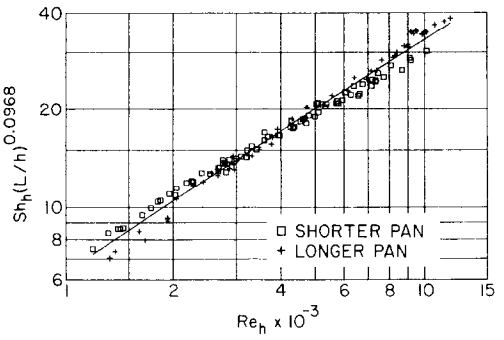

FIG. 4. Modification of the Sh_h–Re_h correlation via the factor $(L/h)^m$.

of the data fall within 5% of the line, and all the data are contained within a $\pm 10\%$ band around the line.

From a comparison of Figs. 3 and 4, it is seen that the greater uniformity of the correlation displayed in the latter is achieved at the price of a somewhat greater spread of the data in the range of larger Re_h. Therefore, although equation (20) provides the best overall representation of the data, equation (19) is a better representation for $Re_h > 3800$.

The correlations thus far presented are to be employed to predict Sherwood numbers within the ranges for which data were collected, namely, Re_h between 1200 and 12,000, and L/h between 8 and 55. In addition, by making use of the analogy between heat and mass transfer, Nusselt numbers can also be predicted. In particular, if $Pr^{0.4}$ and $Sc^{0.4}$ scaling rules are applied for heat and mass transfer, then

$$Nu_h = Sh_h(Pr/Sc)^{0.4}. \tag{21}$$

In applying equation (21), it is relevant to note that $Sc = 0.6$ for the present Sh_h data.

The role played by the step height h as the dominant characteristic dimension in equations (19) and (20) suggests that these representations should not be extrapolated to long pans. This is because for sufficiently long pans, a fully developed mass transfer regime will be approached for which the hydraulic diameter of the flow cross-section will serve as the characteristic dimension. In view of this limitation on equations (19) and (20), attention will now be turned to constructing a correlation suitable for extrapolating the present Sherwood number results to pans longer than those used here.

As a guide for constructing such a correlation, reference may be made to the analysis of turbulent mass transfer at one wall of a parallel-plate channel. The envisioned problem is one in which a hydrodynamically developed, turbulent flow is delivered to the mass transfer section. The hydrodynamic development section and the mass transfer section are assumed to have the same cross-sectional dimensions characterized by the hydraulic diameter D. In the mass transfer section, the mass-transfer-active surface is at a uniform partial density, while the other wall of the channel does not participate in the mass transfer process. The just-described model problem is similar to the classical Graetz problem for laminar flow, and a similar method of analysis is used for the two problems, as set forth in ref. [7].

Let Sh_D represent the average Sherwood number for a length L of the mass transfer section [Sh_D is defined by equation (17)], while $Sh_{D,fd}$ will denote the fully developed Sherwood number. For L/D sufficiently large, it is shown in ref. [7] that

$$Sh_D/Sh_{D,fd} = 1 + C_1/(L/D). \tag{22}$$

In view of the downstep at the beginning of the mass transfer section in the experimental setup, it is appropriate to modify equation (22) by introducing a virtual origin for L. Since the virtual origin is directly related to the step height h, equation (22) is rewritten as

$$Sh_D/Sh_{D,fd} = 1 + C_1 D/(L - C_2 h). \tag{23}$$

For the fully developed Sherwood number, the well-established Petukhov–Popov correlation will be employed

$$Sh_{PP} = Re_D Sc(f/8)/[1.07 + 12.7(f/8)^{1/2}(Sc^{2/3} - 1)] \tag{24}$$

$$f = [1.82(\log Re_D) - 1.64]^{-2}. \tag{24a}$$

As originally formulated, the Petukhov–Popov correlation was for uniformly heated, circular tubes. The use of the hydraulic diameter D should enable the correlation to be applied to rectangular ducts. However, for the one-sided transfer and the uniform partial-density boundary condition of the present experiments, $Sh_{D,fd}$ should be somewhat smaller than the Petukhov–Popov result. With this, equation (23) is recast in the form

$$Sh_D = C_3[1 + C_1 D/(L - C_2 h)]Sh_{PP}. \tag{25}$$

The constants C_1, C_2 and C_3 were chosen to yield the best fit between equation (25) and the experimental data for the longer pan, with the result

$$C_1 = 4.536, \quad C_2 = 6.111, \quad C_3 = 0.898. \tag{25a}$$

The data for the shorter pan were not used in the determination of C_1, C_2 and C_3 because an extrapolation was being sought for pans longer than the longest pan used here.

The quality of the correlation expressed by equations (25) and (25a) is displayed in Fig. 5. On the ordinate, the quantity $Sh_D/[1 + C_1 D/(L - C_2 h)]$ has been plotted, while the abscissa is Re_D. The solid line appearing in the figure represents equation (25) with C_1, C_2 and C_3 from equation (25a). Two-thirds of the data appearing in the figure fall within 2.6% of the correlating line, and the extreme deviation of the data from the line is about 10%.

Equations (25) and (25a) represent the sought-for extrapolation formula. It was derived for $L/h \geqslant 18$, $L/D \geqslant 23.8$, and Re_D between 6400 and 20,000. Moderate extensions of these parameter ranges are

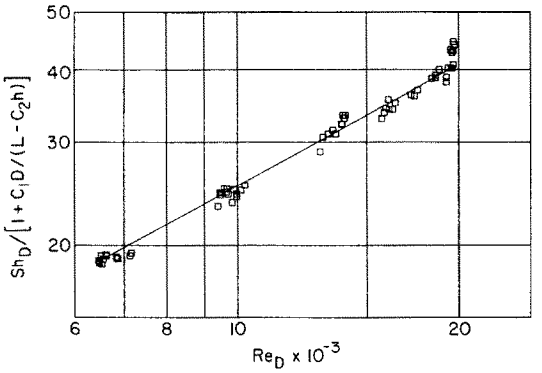

FIG. 5. Sherwood–Reynolds correlation suitable for extrapolation to operating conditions for pans longer than those of the present experiments.

believed admissible. The correlation can be applied directly to heat transfer by replacing *Sh* with *Nu* and *Sc* with *Pr*.

CONCLUDING REMARKS

The experiments performed here have yielded Sherwood numbers for evaporative mass transfer from partially filled pans of distilled water situated in the floor of a flat rectangular duct through which turbulent air flow was passed. The experimental results were generalized in several ways. First, a tight correlation of the Sherwood numbers was achieved for the range of operating conditions that was investigated. This correlation can serve as an interpolation formula among the discrete values of the parameters employed in the experiments. Second, guided by analytical considerations, a correlation was constructed which provides predictions for the Sherwood number for operating conditions corresponding to pans longer than those used in the present investigation. Finally, by making use of the analogy between heat and mass transfer, it was shown how Nusselt numbers can be obtained from the Sherwood number correlations.

REFERENCES

1. R. A. Seban and J. Fox, Heat transfer to the air flow in a surface cavity, *International Developments in Heat Transfer*, Part II, pp. 426–431. American Society of Mechanical Engineers, New York (1962).
2. J. Fox, Heat transfer and air flow in a transverse rectangular notch, *Int. J. Heat Mass Transfer* **8**, 269–279 (1965).
3. R. A. Seban, Heat transfer and flow in a shallow rectangular cavity with subsonic turbulent air flow, *Int. J. Heat Mass Transfer* **8**, 1353–1368 (1965).
4. R. L. Haugen and A. M. Dhanak, Heat transfer in turbulent boundary layer separation over a surface cavity, *J. Heat Transfer* **89**, 335–340 (1967).
5. H. Yamamoto, N. Seki and S. Fukusako, Forced convection heat transfer on a heated bottom surface of a cavity with different wall heights, *Wärme- u. Stöffubertr.* **17**, 73–83 (1983).
6. H. Yamamoto, N. Seki and S. Fukusako, Forced convection heat transfer on heated bottom surface of a cavity, *J. Heat Transfer* **101**, 475–479 (1979).
7. W. Chuck, Evaporation of water from a recessed surface to a parallel forced convection airflow. Ph.D. thesis, Department of Mechanical Engineering, University of Minnesota, Minneapolis, MN (1985).
8. W. C. Reynolds and H. C. Perkins, *Engineering Thermodynamics*, 2nd edn. McGraw-Hill, New York (1977).
9. *ASHRAE Handbook of Fundamentals*, Section 3, p. 2. American Society of Heating, Refrigerating, and Air Conditioning Engineers, Atlanta, GA (1981).

TRANSFERT MASSIQUE PAR EVAPORATION DANS DES ECOULEMENTS TURBULENTS DE CONVECTION FORCEE DANS DES CANAUX

Résumé—Des expériences veulent déterminer les caractéristiques du transfert massique par évaporation à partir de bacs remplis d'eau distillée placés dans le plancher d'un canal rectangulaire traversé par un écoulement d'air turbulent. Pendant les expériences, des variations paramétriques sont faites sur le nombre de Reynolds de l'écoulement d'air, la longueur longitudinale du bac et la distance entre le sommet du bac et la surface libre de l'eau (par la suite appelée la hauteur d'échelon). Pour toutes les conditions opératoires, les nombres de Sherwood mesurés sont très bien unifiés à l'aide du nombre de Reynolds tant que la hauteur d'échelon est prise comme dimension caractéristique. A partir de considérations analytiques une seconde corrélation est établie qui fournit la prévision du nombre de Sherwood pour des conditions correspondant à des bacs plus longs que ceux utilisés dans ces expériences. En appliquant l'analogie entre les transferts de masse et de chaleur, on montre comment les nombres de Nusselt peuvent être obtenus à partir des nombres de Sherwood.

STOFFÜBERGANG DURCH VERDUNSTUNG BEI ERZWUNGENER KONVEKTION IN TURBULENTEN ROHRSTRÖMUNGEN

Zusammenfassung—Es werden Experimente zur Bestimmung des Stoffübergangsverhaltens bei der Verdunstung an teilweise mit destilliertem Wasser gefüllten Wannen durchgeführt, die in den Boden eines flachen rechtwinkligen Kanals eingelassen sind. Im Kanal herrscht turbulente Luftströmung. Bei den Experimenten wurden die Reynolds-Zahl der Luftströmung, die Länge der Wannen in Strömungsrichtung und der Abstand zwischen Wannenoberkante und Wasseroberfläche (künftig als Stufenhöhe bezeichnet) variiert. Bei allen Betriebszuständen konnte die durch Messungen bestimmte Sherwood-Zahl gut mit

der Reynolds-Zahl korreliert werden, vorausgesetzt die Stufenhöhe wurde als charakteristische Länge verwendet. Durch analytische Betrachtungen wurde eine zweite Korrelationsgleichung zur Berechnung der Sherwood-Zahl für Betriebszustände an Wannen, die größer sind als die in den vorliegenden Experimenten verwendeten, aufgestellt. Unter Verwendung der Analogie zwischen Wärme- und Stofftransport kann gezeigt werden, wie Nusselt-Zahlen aus den Korrelationen für die Sherwood-Zahl gewonnen werden können.

МАССОПЕРЕНОС В ПРОЦЕССЕ ИСПАРЕНИЯ ПРИ ТУРБУЛЕНТНОМ ТЕЧЕНИИ С ВЫНУЖДЕННОЙ КОНВЕКЦИЕЙ В ТРУБЕ

Аннотация—Выполнены эксперименты по определению характеристик массопереноса при испарении из частично заполненных дистиллированной водой плоских углублений в днище прямоугольного канала, через который пропускался турбулентный поток воздуха. В ходе экспериментов изменялись число Рейнольдса для потока воздуха, длина плоского углубления и расстояние между высотой углубления и поверхностью воды (называемое в дальнейшем высотой уступа). При всех режимных условиях проведения эксперимента измеренные значения числа Шервуда хорошо коллелировались со значениями числа Рейнольдса, когда высота уступа использовалась в качестве характерного размера. На основе аналитических расчетов предложено еще одно критериальное соотношение, позволяющее определять числа Шервуда для более протяженных углублений. На основе аналогии между переносом тепла и массы показана возможность определения чисел Нуссельта из соотношений для числа Шервуда.